

MEMORANDUM

To: Herb Freese and Dave Rubenstien (Science Applications International, Corp., McLean, VA), Mike Porter (SAIC, San Diego, CA)
From: Richard Evans (SAIC, New London, CT)
Subject: Calculation of internal wave eigen-frequencies and modes; Displacement and sound speed realizations
Date: November 30, 2000

Introduction:

The stability of procedures for finding internal wave eigenvalues and modes can present an obstacle to the simulation of sound speed variations caused by internal waves. This problem can be overcome by an adaptation of the techniques used in the acoustic normal mode program Kraken [1] that are described in this memo. The techniques are a finite difference approximation of the applicable differential equation, the application of the Sturm sequence [2] and bisection to find the eigenvalues, and inverse iteration to find the eigenvectors or modes.

Once the internal wave eigenvalues and modes are found, they can be used to generate realizations of displacements caused by the internal wave. A procedure to generate displacements with statistics provided by the Garrett-Munk power spectrum [3] is described in this memo along with a formula of Munk and Zachariasen [4] for converting the displacements into sound speed realizations.

These procedures have been implemented in a Fortran computer program called Wave. Sample results are presented to complement the description of the computational techniques.

Internal Wave Eigenvalues and Modes:

The internal wave eigenvalues and modes are determined by the water depth H in meters and the buoyancy frequency profile $N(z)$ and inertial frequency ω_I in rad/s. The internal wave modes $W_j(z)$ satisfy the eigenvalue problem

$$\frac{d^2 W_j(z)}{dz^2} + \left[\gamma_j^2 \left[N^2(z) - \omega_I^2 \right] - k^2 \right] W_j(z) = 0 \quad (1)$$

where $W_j(0) = W_j(H) = 0$ and k is a known spatial wave number in rad/m. The quantities $\gamma_j^2, j = 1, J$ are the eigenvalues that are related to the eigen-frequencies by the equation $\omega_j^2 = \omega_I^2 + k^2 / \gamma_j^2$ [5]. The internal wave modes are normalized so that

$$\int_0^H \left[N^2(z) - \omega_I^2 \right] W_j(z) W_{j'}(z) dz = \delta_{j,j'}. \text{ The weight function } N^2(z) - \omega_I^2, \text{ which}$$

multiplies the eigenvalue in Eq. (1), is assumed to be positive. An alternative formulation of the internal wave boundary value problem, which treats the temporal frequency ω as

known and attempts to find a discrete set of spatial wave numbers k as eigenvalues, has a weight function that can be both positive and negative. This form is not suitable for the Sturm sequence method.

A finite difference approximation of the eigenvalue problem in Eq. (1) is obtained by dividing the interval $[0, H]$ into N parts of size $\Delta z = H/N$. First restate Eq. (1), suppressing the dependence on j , as

$$\frac{d^2 w(z)}{dz^2} + \left[\lambda b^2(z) - k^2 \right] w(z) = 0 \quad (2)$$

where $w(0) = w(H) = 0$, $b^2(z) = N^2(z) - \omega_l^2$ and $\lambda = \gamma^2$. Then by defining $b_n^2 = b^2(n\Delta z)$ and $w_n = w(n\Delta z)$ for $n = 0, N$ and applying three point central differencing to Eq. (2) one obtains

$$-w_{n+1} + (2 + \Delta z^2 k^2) w_n - w_{n-1} = \lambda \Delta z^2 b_n^2 w_n, \quad n = 1, N - 1 \quad (3)$$

where $w_0 = w_N = 0$.

A matrix equation, of the form $Aw = \lambda B^2 w$, is obtained from Eq. (3) for the column vector $w = \text{col}(w_n, n = 1, N - 1)$. The matrix equation is brought into standard form by multiplying on the left by B^{-1} to obtain $(B^{-1}AB^{-1})Bw = \lambda Bw$ and defining the new vector $u = Bw$. The standard form is $Cu = \lambda u$ where $C = B^{-1}AB^{-1}$. The assumption that the weight function is positive is critical to this step, since the entries in the diagonal matrix B^{-1} are $1/\sqrt{\Delta z^2 b_n^2} = 1/(\Delta z b_n)$, $n = 1, N - 1$.

The diagonal entries in the tridiagonal matrix C are $c_{n,n} = (2 + \Delta z^2 k^2)/(\Delta z^2 b_n^2)$, $n = 1, N - 1$ while the superdiagonals and subdiagonals are $c_{n-1,n} = c_{n,n-1} = -1/(\Delta z^2 b_n b_{n-1})$, $n = 2, N - 1$. The symmetric tridiagonal matrix $C - \lambda I$ is suitable for the application of the Sturm sequence, which is a stable recursion for its determinant. Overflow and underflow are avoided, in the recursion, by applying the roof and floor logic (scaling) from Kraken. The zeroes of the determinant of the matrix $C - \lambda I$ approximate the eigenvalues of Eq. (1).

The eigenvalues of Eq. (1) are bounded below by $k^2 / \max[N^2(z) - \omega_l^2]$ as can be established using an extension of the argument in [6]. The eigenvalues are found by starting at $k^2 / \max[N^2(z) - \omega_l^2]$, taking small steps of size $\Delta \lambda$ until a zero crossing of $\det[C - \lambda I]$ is found, and then applying bisection [7]. The value $\Delta \lambda = .1 \text{ (s/m)}^2$ seems to work well, for the examples considered so far. The process is repeated until J eigenvalues $\lambda_j \cong \gamma_j^2$, $j = 1, J$ are found.

The eigenvectors u_j corresponding to λ_j are found by inverse iteration. Given almost any vector $\vec{v} = \sum_{m=1}^J a_m \vec{u}_m$, then $[C - (\lambda_j - \varepsilon)I]^{-1} \vec{v} = \sum_{m=1}^J \frac{a_m}{\lambda_m - (\lambda_j - \varepsilon)} \vec{u}_m \cong \frac{a_j}{\varepsilon} \vec{u}_j$ where ε can be quite small. Hence, solving the tridiagonal matrix equation $[C - (\lambda_j - \varepsilon)I]v_i = v_{i-1}$ for several iterations will bring out the eigenvector u_j , with some scaling factor. The eigenfunctions, on the depth grid, are found using $w_j = B^{-1}u_j, j = 1, J$. They must be normalized to obtain $W_j, j = 1, J$.

Displacements:

The complex internal wave displacements, with real and imaginary parts in meters, are taken to have the form [5]

$$\xi(r, z, t) = \sum_{j=1}^J \int_{-\infty}^{+\infty} A_j(k) W_j(k^2, z) \exp[ikr + i\omega_j(k^2)t] dk \quad (4)$$

where the k^2 dependence of the internal wave modes and eigen-frequencies are indicated explicitly. The expansion coefficients $A_j(k)$ are identically distributed complex Gaussian random variables with zero mean. Their variance is given by the Garrett-Munk power spectrum defined in Flatte', et. al. [3] as

$$P_j(k^2) = E_0 \frac{4}{\pi^2} \frac{3}{j^2 + 9} \frac{k_j k^2}{(k^2 + k_j^2)^2} \quad (5)$$

where $k_j = (\pi F_I / BN_0)j$, $B=1300$ m, $N_0 = 3$ cycles/hour and $E_0 = 4.0$. The quantity F_I is the inertial frequency computed using $F_I = (1/12) \sin(\text{latitude})$ with units of cycles/hour. The power spectrum is normalized so that

$$\sum_{j=1}^J \int_{-\infty}^{+\infty} P_j(k^2) dk \cong E_0 ,$$

for large J , where the energy density factor E_0 is chosen to yield a depth integrated value of 4.0×10^3 Joules/m² with a seawater density of 1.0×10^3 kg/m³. E_0 is divided by the density because the density is not included in the normalization of the internal wave modes as it is in Flatte', et. al. [3].

A calculation of internal wave displacements requires a numerical approximation of integral in Eq. (4). This starts with a choice of a maximum wave number k_{\max} to bound the interval that contains the majority of the energy in the internal wave spectrum. For the Garrett-Munk power spectrum this is around .5 cycles/km converted into rad/m. The interval $[0, k_{\max}]$ is divided into M parts of size $\Delta k = k_{\max} / M$. The discrete horizontal wave numbers, used in the internal wave eigen-frequency calculations, are

taken to be $k_m = m\Delta k$, $m = 1, M$. The integral in Eq. (4) is approximated, using both positive and negative values of m , by

$$\xi(r, z, t) \cong \sum_{j=1}^J \sum_{m=\pm 1}^{\pm M} \sqrt{\frac{P_j(k_m^2)}{\Delta k}} G_{j,m} W_j(k_m^2, z) \exp[ik_m r + i\omega_j(k_m^2)t] \Delta k \quad (6)$$

where both the real and imaginary parts of $G_{j,m}$ are Gaussian random variables with zero mean and unit variance. Independent realizations of $G_{j,m}$ are generated by calling the subroutine ‘‘GASDEV’’ [8] separately for the real and imaginary parts and for each j and m (both positive and negative).

Verification of the amount of energy in the internal wave field is an important check. It is confirmed by showing that the depth integrated energy density satisfies

$$\int_0^H [N^2(z) - \omega_l^2] \langle \xi(r, z, t) \xi^*(r, z, t) \rangle dz \cong 2E_0 \quad .$$

The superscript asterisk stands for complex conjugation and the factor of 2 occurs because both real and imaginary parts of the displacement are included. The angular brackets represent an ensemble average over realizations of displacement. Substitution of Eq. (6) into the ensemble average gives

$$\langle \xi(r, z, t) \xi^*(r, z, t) \rangle \cong \sum_{j,j'=1}^J \sum_{m,m'=\pm 1}^{\pm M} \sqrt{P_j(k_m^2) P_{j'}(k_{m'}^2)} \langle G_{j,m} G_{j',m'}^* \rangle W_j(k_m^2, z) W_{j'}(k_{m'}^2, z) \times \\ \exp\{i[k_m - k_{m'}]r + i[\omega_j(k_m^2) - \omega_{j'}(k_{m'}^2)]t\} \Delta k \quad .$$

The independence of the $G_{j,m}$ yields $\langle G_{j,m} G_{j',m'}^* \rangle = \delta_{j,j'} \delta_{m,m'}$ and consequently

$$\langle \xi(r, z, t) \xi^*(r, z, t) \rangle \cong 2 \sum_{j=1}^J \sum_{m=\pm 1}^{\pm M} P_j(k_m^2) W_j^2(k_m^2, z) \Delta k \quad .$$

Evaluating the depth integrated energy density gives

$$\int_0^H [N^2(z) - \omega_l^2] \langle \xi(r, z, t) \xi^*(r, z, t) \rangle dz \cong 2 \sum_{j=1}^J \sum_{m=\pm 1}^{\pm M} P_j(k_m^2) \Delta k \cong 2E_0$$

because of the modal normalization and the normalization of the Garrett-Munk power spectrum.

Sound Speed Fluctuations:

The displacement fields obtained from Eq. (6) are converted into sound speed fluctuations using the relation from Munk and Zachariasen [2]

$$\delta c(r, z, t) \cong (dc_p / dz) \text{Re}[\zeta(r, z, t)] \quad (7)$$

where dc_p / dz is the potential sound speed gradient in (m/s)/m. The potential sound speed gradient is computed from the temperature and salinity profile, and the equation for sound speed, using

$$\frac{dc_p}{dz} = \frac{\partial c}{\partial T} \left(\frac{dT}{dz} - \frac{dT_a}{dz} \right) + \frac{\partial c}{\partial S} \frac{dS}{dz}$$

It depends on the adiabatic temperature gradient dT_a / dz , the gradients of temperature T and salinity S with respect to depth, and the partial derivatives of sound speed c with respect to temperature and salinity. Also see pg. 4-5 in Flatte', et. al. [3].

Example:

A computer program called Wave performs the calculations described in the last three sections. The inputs and outputs are described in an ASCII text file called Wave.txt that accompanies the Fortran source code. This section provides the results of a sample calculation for a temperature and salinity profile (called #336) taken from the North Pacific in a water depth of 4100 meters. The temperature and salinity was provided at 26 depths and most of the samples were in the upper 1000 m of the water column.

The buoyancy frequency profile was generated on a uniform mesh, with a depth increment of $\Delta z = 2$ m, for the purpose of computing the internal wave modes and eigen-frequencies. The top 1000 m of the buoyancy frequency profile is shown in Fig. 1, with a peak at about 120 m. A wave number sampling increment of $\Delta k = .01$ cycles/km was used with 50 samples between .01 and .5 cycles/km and another 50 at negative wave numbers. A total of 20 internal wave modes and eigen-frequencies were computed at each of the 50 positive wave numbers. The dispersion relations, between the wave numbers and eigen-frequencies, are plotted in Fig. 2.

An energy density factor of $E_0 = 4$ was used to generate realizations of displacements. Sound speed profiles were obtained by adding the fluctuations in Eq. (7) to the background sound speed profile, computed from the temperature and salinity. Sound speed profiles were generated every 600 s between 0 and 3000 s and every .1 km between 0 and 9 km. The temporal dependence of the sound speed is shown in Fig. 3, for a single realization of the internal wave field. The spatial dependence is shown in Fig. 4.

The range dependence of the sound speed profile is the most important consequence, of the internal waves, on the temporal and spatial scales selected. The effects are confined to the top 200 m of the water column in this case.

Acknowledgment:

This work was supported by The National Defense Center of Excellence for Research in Ocean Sciences (CEROS), Maui, HI. Thanks to CEROS and Mike Porter for the encouragement.

References:

1. M. Porter, "The KRAKEN normal mode program," Saclantcen Memorandum, SM-245 (SACLANT Undersea Research Centre, LaSpezia, Italy, September 1991).
2. J. H. Wilkinson, **The Algebraic Eigenvalue Problem**, p. 300 (Oxford Univ. Press, 1965).
3. M. Flatte', R. Dashen, W. H. Munk, K. W. Watson and F. Zachariasen, **Sound Transmission through a Fluctuating Ocean**, pp. 56-57 (Cambridge Univ. Press, 1979).
4. W. H. Munk and F. Zachariasen, "Sound propagation through a fluctuating ocean: Theory and observation," J. Acoust. Soc. Am. 59, 818-838 (1976)
5. L. B. Dozier and F. D. Tappert, "Statistics of normal mode amplitudes in a random ocean. I. Theory," J. Acoust. Soc. Am. **63**, 353-365 (1978).
6. R. B. Evans, "The existence of generalized eigenfunctions and multiple eigenvalues in underwater acoustics," J. Acoust. Soc. Am. **92**, 2024-2029 (1992).
7. B. Carnahan, H. A. Luther and J. O. Wilkes, **Applied Numerical Methods**, p. 185 (Wiley, New York, 1969)
8. W. H. Press, S. A. Teukolsky, W. T. Vetterling and B. P. Flannery, **Numerical Recipes in Fortran, Second Edition**, pp. 463-475 (Cambridge Univ. Press, New York, 1992)

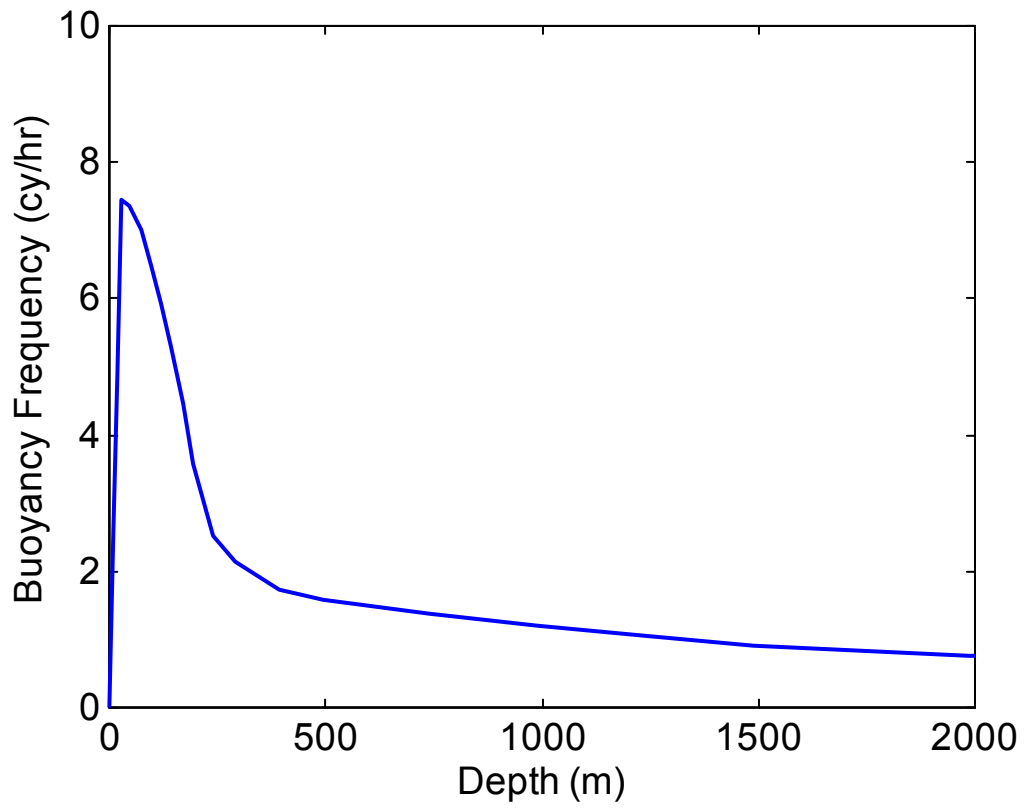


Figure 1. Buoyancy frequency profile

11/22/06

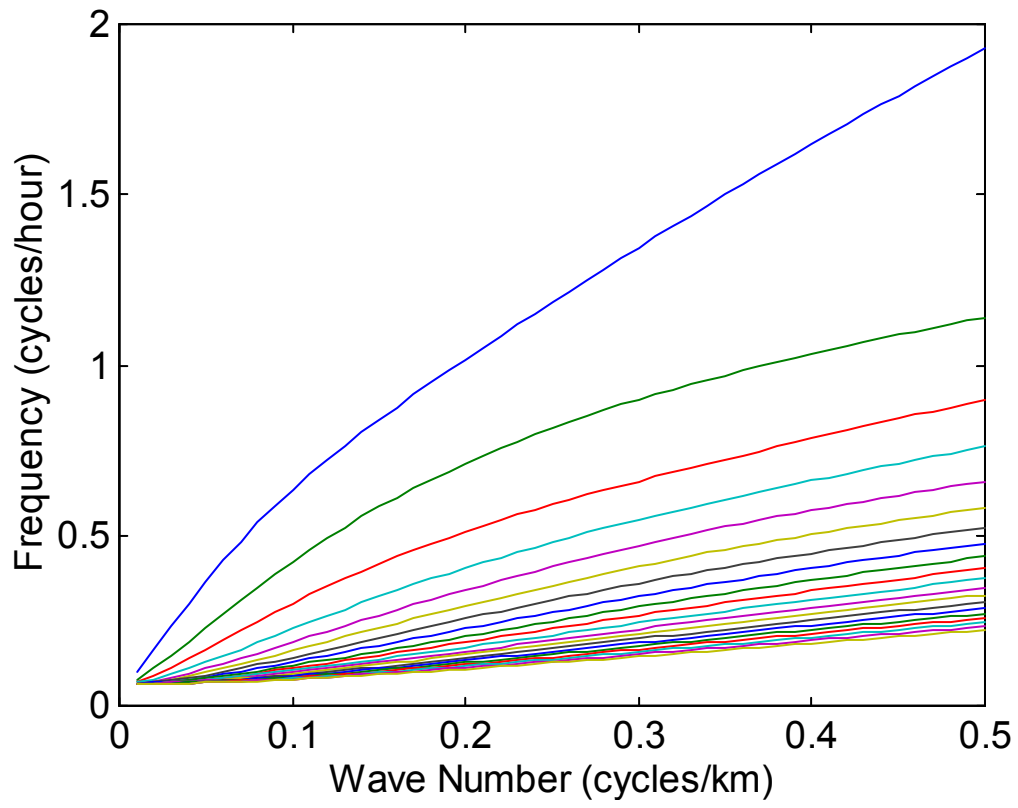


Figure 2. Internal wave dispersion relations

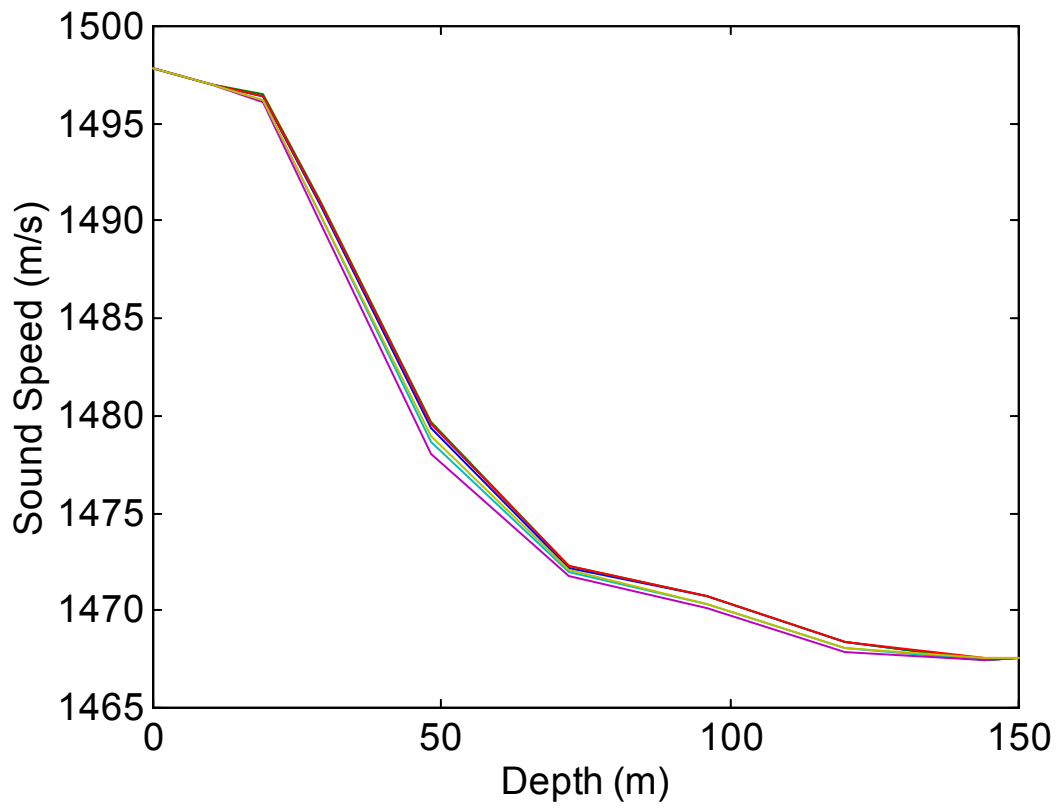


Figure 3. Six sound speed realizations in 50 minutes, ten minutes apart.

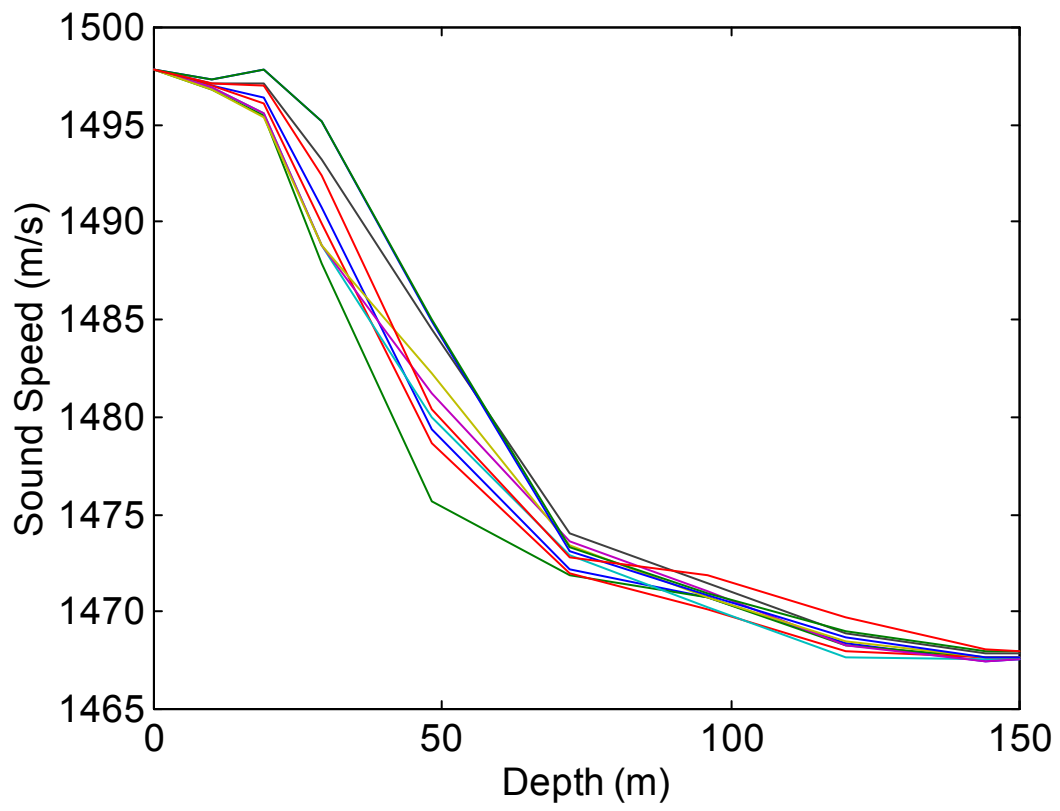


Figure 4. Ten sound speed realizations in 9 km, .1 km apart.